TISSUE ENGINEERING: Part A
Volume 00, Number 00, 2024

DOI: 10.1089/ten.tea.2024.0064

ORIGINAL ARTICLE

Incorporating Microbial Stimuli for Osteogenesis in a Rabbit Posterolateral Spinal Fusion Model

Nada Ristya Rahmani, MD,[1,2] Anneli Duits, MD,[1] Michiel Croes, PhD,[1] Olivia Lock, BSc,[1] Debby Gawlitta, PhD,[2,3] Harrie Weinans, PhD,[1,4] and Moyo C. Kruyt, PhD[1,5]

Autologous bone grafts are commonly used to repair defects in skeletal tissue, however, due to their limited supply there is a clinical need for alternatives. Synthetic ceramics present a promising option but currently lack biological activity to stimulate bone regeneration. One potential approach to address this limitation is the incorporation of immunomodulatory agents. In this study, we investigate the application of microbial stimuli to stimulate bone formation. Three different microbial stimuli were incorporated in a biphasic calcium phosphate (BCP) ceramic: Bacille Calmette–Guérin (BCG), gamma-irradiated *Staphylococcus aureus (*γi-*S. aureus)*, or γi-*Candida albicans* (γi-*C. Albicans*). The constructs were then implanted in both a rabbit posterolateral spinal fusion (PLF) and an intramuscular implant model for 10 weeks and compared to a nonstimulated control construct. For the PLF model, the formation of a bony bridge was evaluated by manual palpation, micro computed tomography, and histology. While complete fusion was not observed, the BCG condition was most promising with higher manual stiffness and almost twice as much bone volume in the central fusion mass compared to the control (9 ± 4.4% bone area vs. 4.6 ± 2.3%, respectively). Conversely, the γi-*S. aureus* or *γi-C. albicans* appeared to inhibit bone formation (1.4 ± 1.4% and 1.2 ± 0.6% bone area). Bone induction was not observed in any of the intramuscular implants. This study indicates that incorporating immunomodulatory agents in ceramic bone substitutes can affect bone formation, which can be positive when selected carefully. The readily available and clinically approved BCG showed promising results, which warrants further research for clinical translation.

Keywords: osteoimmunomodulation, ceramic, fungi, bacteria, mycobacterium, bone regenerative medicine

Impact Statement

Inflammatory signals play an important role in bone repair and regeneration. Here we demonstrate the feasibility of applying microbial stimuli as a bioactive agent to promote bone regeneration in a relevant preclinical animal model.

[1]Department of Orthopedics, University Medical Centre Utrecht, Utrecht, The Netherlands.
[2]Regenerative Medicine Centre Utrecht, University Medical Centre Utrecht, Utrecht, The Netherlands.
[3]Department of Oral and Maxillofacial Surgery, Prosthodontics and Special Dental Care, University Medical Centre Utrecht, Utrecht, The Netherlands.
[4]Department of Biomechanical Engineering, Technical University Delft, The Netherlands.
[5]Department of Developmental Biomedical Engineering, Twente University, Enschede, The Netherlands.

Introduction

Bone is the second most transplanted tissue after blood. Bone grafting is a common procedure for treating defects in the skeletal system caused by trauma, tumor resection, and more. Autologous bone has the ideal properties to be used as a bone graft, however, the availability is limited and its harvesting prolongs surgical time.[1] Synthetic ceramics that mimic the inorganic components of bone are increasingly used as a substitute for bone grafts. They are well known for their osteoconductive properties, biocompatibility, and long shelf-life.[2] A recent clinical trial demonstrated that microporous biphasic calcium phosphate (BCP) ceramics had a similar success to autograft in a stand-alone instrumented posterolateral spinal fusion (PLF) study, with a fusion rate of 55% compared with 52% for autograft at 1-year follow-up.[3] Although this is promising, a 100% fusion should be the aim and therefore, the hunt for further optimization of the graft substitute continues. This may be accomplished with the next generation of calcium phosphate ceramics with submicron surface topography that was found to better induce new bone in an ectopic implant animal model.[4] For this material, its specific interaction with immune cells, such as macrophages, was hypothesized to be associated with the *de novo* bone formation.[4–6] Modulating the interaction between a biomaterial and immune cells to stimulate bone formation has become a growing area of interest.[7–9] Although short-lived, the initial inflammatory reaction toward a biomaterial can significantly impact its long-term performance and integration with the host tissue.[10]

The implantation of a biomaterial initially triggers inflammation. This response determines the type of tissue that will form and at which speed. In the context of bone repair and regeneration, a well-sequenced inflammation plays a critical role in the process of osteoinduction,[11] which refers to the induction of undifferentiated progenitor cells such as mesenchymal stromal cells (MSCs) into the osteogenic lineage.[12] The inflammatory niche provides signaling molecules and chemokines that activate and attract local quiescent and distant MSCs.[13–15] The concentration of relevant growth factors increases during the inflammatory stage, which normally, under homeostatic conditions are tightly regulated.[16,17] Moreover, immune cells such as macrophages are among the main source of these growth factors.[18] Inflammation also supports bone repair by triggering the formation of new blood vessels, by molecules such as vascular endothelial growth factor and fibroblast growth factor.[19]

On the contrary, the inflammatory response can also inhibit bone formation, for example during prolonged or chronic inflammation, as a response to an infection or to wear particles from polymeric or metal implants.[20] While proinflammatory signals can initiate the differentiation of MSCs, it is an anti-inflammatory environment that facilitates the maturation of differentiated osteoblasts. This allows cells to deposit osteoid, which eventually becomes a mineralized bone matrix.[21] Much is still unknown regarding the precise sequence and optimal range of pro- or anti-inflammatory factors required for effective new bone formation. However, former research demonstrated achieving a balanced inflammation and timing is important in this process.[14]

In a previous study, we successfully applied inactivated microbe-derived agents as a proinflammatory strategy to enhance osteogenesis in a rabbit tibia model.[22,23] After 8 weeks, gamma-irradiated *Staphylococcus aureus* (γi-*S. aureus*) led to significant thickening of the tibial cortex with none to minimal lytic lesions, predominantly showing a healthy bone structure. Similar findings were observed for γi-*Escherichia coli* and γi-*Mycobacterium marinum* although not as robust as with γi-*S. aureus.* In agreement, the application of microbial-derived agents for bone and dental implants was also reported by Shi *et al.* who prepared a polysaccharide fungal component, zymosan, as a coating on titanium substrates that demonstrated improvement in the osseointegration of the coated implant in a rat femur condyle defect model compared with the uncoated control.[24]

To take these findings further, we explore the potential of microbe-derived stimuli to improve the osteogenesis of ceramic bone graft substitutes in a preclinical orthopedic model. Specifically, we examined the pro-osteogenic effect of the incorporation of γi-*S. aureus*, γi-*Candida albicans* (γi-*C. albicans*), and BCG in BCP scaffold with submicron surface topography.[25] BCG is included in the study as it is an available medicinal product containing attenuated bacterium (*Mycobacterium bovis*). The ceramics treated with the different microbial stimuli were studied in the well-established rabbit PLF model to assess the efficacy of bone graft substitutes.[26–28] In addition, the ability to induce new bone formation was investigated in an intramuscular ectopic implant model. The findings of this study could have important implications for the development of new and improved therapies for bone regeneration and repair.

Materials and Methods

Materials

Three different microbes were tested in this study: *S. aureus* (Wood 46, ATCC 10832), *C. albicans* (ATCC 10231), and BCG. *S. aureus* and *C. albicans* were obtained from cultures of the microbiology department of Utrecht University in lysogeny broth medium at 37°C to mid-log phase, aliquoted and stored at −80°C in phosphate-buffered saline (PBS) with 40% (v/v) glycerol. Cultured microbes were killed by γi at 25 kGy (Steris AST, Ede, The Netherlands), which is the standard dose for sterilization of medical and biological products.[29] BCG (Lamepro, The Netherlands) was obtained from the pharmacy department of the University Medical Center Utrecht.

Commercially available BCP (MagnetOs©; Kuros Biosciences BV, Bilthoven, The Netherlands) in the form of granules (1–2 mm) and cylindrical discs (9 mm Ø; 6 mm height) were used as a scaffold. The BCP consisted of 65–75% tricalcium phosphate [TCP—$Ca_3(PO_4)_2$] and 25–35% hydroxyapatite [HA—$Ca_{10}(PO_4)_6(OH)_2$] with a submicron needle-shaped surface topography (average crystal diameter of 0.58 ± 0.21 μm).[25] BCP scaffolds were sterilized by autoclaving at 121°C and dried at 60°C.

Whole-blood assay

The extent of the rabbit's immune response toward different concentrations of microbial stimuli was studied in a whole-blood assay prior to the surgical intervention. Peripheral blood was collected sterilely from 5 animals in a sodium heparin-coated tube. The blood was diluted 1:5 with a culture medium containing RPMI (Gibco, 1640)

100 U/mL penicillin, and 100 U/mL streptomycin (Gibco). A 48-well plate (300 μL/well) was used for the experiment, which consisted of 270 μL of diluted blood and 30 μL of concentrated microbial stimuli in PBS. The groups tested were BCG (1×10^3–1×10^6 units/mL), γi-*S. aureus* (1×10^4–1×10^7 units/mL), and γi-*C. albicans* (1×10^4–1×10^7 units/mL). Lipopolysaccharide (0.1–100 ng/mL) was used as a positive control. The blood was stimulated for 24 h at 37°C and 5% CO_2. Afterward, the plate was centrifuged at 500 ×*g* for 10 min at 4°C. The clear supernatant was collected and stored at −80°C until analysis. Cytokine levels of interleukin (IL)-6 and IL-1β were measured as indicators of a proinflammatory reaction using the Rabbit DuoSet® ELISA kits (R&D Systems, the Netherlands) according to the manufacturer's protocol.

Implant preparation

Spinal fusion implants. BCP granules were sterilized by autoclaving and prepared max 1 week before surgery. In a 6-well plate, 2 cc of BCP were mixed with 2 mL of microbial stimuli (diluted in PBS), then placed on a plate shaker for 1 h at 50 rpm. The concentration of microbial stimuli tested *in vivo* was 2×10^6 units/mL for BCG and γi-*S. aureus*; and 2×10^7 for γi-*C. albicans*. Excess liquid was aspirated from the wells and the granules were air dried overnight. Subsequently, the treated BCP granules were transferred to a modified syringe, wherein the nozzle was removed, and a sterile plunger was employed to seal the opening (Fig. 1). BCP was stored at 4°C until the day of surgery. During surgery, blood plasma was used to bind the granules together. For this, 4 mL of autologous blood was collected in a citrate-coated tube and centrifuged at 2000 ×*g* for 10 min at room temperature. Clear plasma (1.2 mL) was mixed thoroughly with 60 μl of 0.5 M calcium chloride dihydrate (Sigma Aldrich). The syringe containing treated BCP granules was opened, supplemented with PBS (500 μL) to provide moisture, and then mixed with the plasma solution. Subsequently, the syringe was placed in an incubator (37°C) for 20–30 min until clotted. All steps were conducted under sterile conditions.

Intramuscular implants. BCP discs were sterilized by autoclaving and prepared max 1 week before surgery by adding 200 μL of microbial stimuli diluted in PBS at high and low concentrations: BCG (1×10^5 and 1×10^6 units/mL), γi-*S. aureus* (1×10^5 and 1×10^6 units/mL), and γi-*C. albicans* (1×10^5 and 1×10^7 units/mL). Treated BCP discs were dried by air-flow overnight and stored at 4°C. All steps were conducted under sterile conditions.

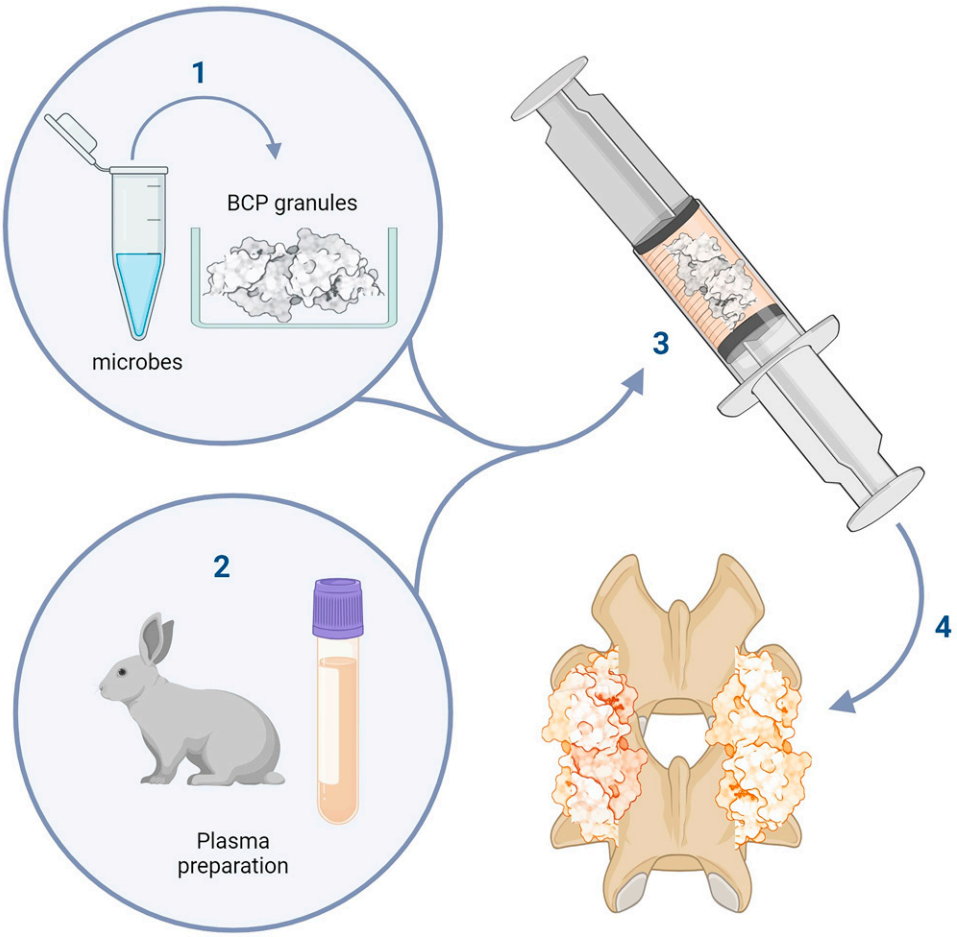

FIG. 1. Schematic overview of the implant preparation. **(1)** Microbial stimuli diluted in PBS were added to BCP granules and dried overnight. **(2)** Blood plasma was collected in a citrate-coated tube and mixed with calcium chloride dihydrate. **(3)** BCP granules were mixed with the plasma solution in a modified syringe and placed at 37°C for 20–30 min for clotting. **(4)** Implantation at the bilateral transverse processes. PBS, phosphate-buffered saline, BCP, biphasic calcium phosphate.

Animal experiment

Twenty-four female New Zealand White rabbits (Crl:KBL, Charles River, France) were used (aged 20–25 weeks, weight 3–4 kg). All procedures were reviewed and approved by the Central Authority for Scientific Procedures on Animals (CCD, protocol number AVD1150002016445) and by the local animal ethics committee. Animals were housed in pairs at room temperature, fed standard rabbit chow, and had access to water *ad libitum*. The animals were acclimatized for 1 week, underwent a daily standard healthcare inspection, and were weighed weekly.

Each rabbit underwent a bilateral, single-level, noninstrumented PLF and implantation of 3 intramuscular implants in the paraspinal muscle. The animals were divided into four groups ($n = 6$): i) no microbial stimulus (control); ii) BCG; iii) γi-*S. aureus*, and iv) *γi-C. albicans*. Table 1 provides a description of the constructs implanted. Each animal received the same microbial stimulus for the spinal and intramuscular procedures. For the intramuscular implants, the conditions included a control (plain BCP), and a high, and low concentration of the microbial stimulus.

Penicillin (4×10^4 mg/kg s.c., Duplocilline®, Merck Animal Health, Madison, USA) was administered once as a prophylactic antibiotic. The rabbits were premedicated with buprenorphine (0.03 mg/kg s.c., Temgesic) and midazolam (0.5 mg/kg i.m.). General anesthesia was induced by etomidate (1.8 mg/kg i.v.) and maintained with sufentanyl (0.037 mg/kg) and isoflurane (2–2.5 mL/h). The rabbit was placed in a prone position. The dorsal skin was shaved and disinfected with povidone-iodine. Because the number of lumbar vertebrae is known to vary between rabbits,[30] the lumbosacral junction was used as an anatomical landmark to determine the PLF level. PLF was conducted across the third intravertebral space cranial to the lumbosacral joint, which is L4–L5 in the majority of animals. Here, a midline skin incision of 5–6 cm was made. About 2 cm bilateral from the midline, the longissimus muscles were separated bluntly until the transverse processes were exposed and cleared. Using a diamond-shaped drill (0.3 cm Ø), the paramedian surface was decorticated under constant cooling with saline until pink bedding of about 1 cm width was seen. Then, the coagulated BCP granules (about 3 cc per side) were placed overlying the transverse processes and intertransverse ligament. The wound was closed in multiple layers using 3-0 absorbable sutures (Vicryl, Ethicon).

Three intramuscular pockets were made, cranial to the PLF levels and approximately 3–4 cm apart, by a small incision of 1 cm in the fascia followed by blunt distraction. Each pocket received a BCP disc and afterward was closed with a single 3-0 absorbable suture. At the end of the surgery, a temperature monitoring chip was inserted subcutaneously. The mean operative time was ±50 min.

After surgery, the rabbits were placed in solitary housing with a heat source overnight before returning to their regular cage. The animals were handled as minimally as possible for 2 weeks by using a transport box to lift rabbits from the cage to aid fusion.[31] Buprenorphine (0.03 mg/kg s.c.; Temgesic) was administered every 12 h for 2 consecutive days as pain management. Fluorochrome labels were administered at 4, 7, and 8 weeks after surgery to detect the dynamics of mineralization, in the following order: oxytetracyline (20 mg/kg s.c.; Engemycin 10%, Mycofarm), calcein green (10 mg/kg s.c.; calcein disodium salt, 21030 Sigma-Aldrich, dissolved in 2% $NaHCO_3$), and xylenol orange (30 mg/kg s.c.; xylenol orange tetrasodium salt, 398187 Sigma Aldrich, dissolved in 1% $NaHCO_3$).

Body temperature was measured daily and body weight weekly to monitor for adverse systemic effects from the intervention. C reactive protein (CRP), a serum acute phase protein secreted by the liver in response to elevated cytokines, was measured prior to surgery and at weeks 3 postsurgery to identify a prolonged inflammatory response. CRP levels on weeks 1 and 2 postsurgery were not considered relevant, as they are typically elevated due to the surgical procedure itself. After 10 weeks, the rabbits were euthanized by a pentobarbital overdose. Samples were harvested and stored in 4% formaldehyde until further analysis.

Serum CRP

Blood (1 mL) was collected from the marginal ear vein of the rabbits in a serum clot activator tube (VACUETTE® CAT, 454098). Blood was left undisturbed at room temperature for 15–30 min until the blood clot was separated from the serum. Serum samples were stored at −20°C until analysis. CRP levels were measured using the Rabbit CRP (PTX1) ELISA Kit (ab157726, Abcam, USA) according to the manufacturer's protocol.

Gross inspection and manual palpation

During the necropsy, the surgical field was examined for complications and the lumbar spine was removed. Manual palpation of the operated level was performed on the freshly

Table 1. Overview of control and experimental groups for both types of implants

		PLF implant			*Intramuscular implant*		
No.	*Group*	*Concentration (units/mL)*	*BCP*	n	*Concentration (units/mL)*	*BCP*	n
i.	Control	—	granules	6	—	disc	6
ii.	BCG	2×10^6	granules	6	High: 1×10^6	disc	6
					Low: 1×10^5	disc	6
iii.	γi-*S. aureus*	2×10^6	granules	6	High: 1×10^6	disc	6
					Low: 1×10^5	disc	6
iv.	γi-*C. albicans*	2×10^7	granules	6	High: 1×10^7	disc	6
					Low: 1×10^6	disc	6

BCP, biphasic calcium phosphate; BCG, Bacille Calmette–Guérin.

obtained specimen. Flexion extension and lateral bending movements were applied to the fusion level and the level of mobility was compared to the nonintervened level. Fusion was graded as not fused, stiff (reduced movement compared with nonintervened levels), or fused (no detectable movement).

Micro computed tomography (micro-CT) imaging

The operated level was scanned in a micro-CT with a tube voltage of 90 kV and a current of 180 μA (Quantum FX, PerkinElmer, Waltham, MA). Images were taken with a voxel size of 40 μm, represented as a stack of 2D TIFF images.

Histology

The samples were embedded undecalcified for hard tissue analysis. The samples were first fixed in 4% (v/v) formaldehyde and dehydrated in an ethanol series. Subsequently, the samples were embedded in methyl methacrylate containing 20% (v/v) plastoid N (Sigma) and 2.8% (w/v) benzoyl peroxide (Luperox, Sigma), then immersed in a water bath until polymerized. Approximately 30 μm-thick sections were made with a Leica 1600 SP saw microtome (Leica, Nussloch, Germany) and stained with basic fuchsin and methylene blue for general histological assessment or left unstained for fluorochrome detection (Thunder imaging, Leica microsystem, Germany). Spinal sections were made mid-sagittal and for the intramuscular implants, transverse sections from the mid-third region of the BCP discs were used for histomorphometry.

Histomorphometry

Sections were digitized using the Leica DMi8 (Thunder) microscope equipped with a DFC9000 camera, operated by LASX software. The various tissue types (bone, bone marrow, fibrous tissue, and scaffold) were pseudo-colored using Adobe Photoshop 2020 (Adobe Systems, San Jose, USA). Area percentage was calculated for the scaffold, bone tissue, and marrow-like structures using the percentage of pixels relative to the region of interest (ROI). The ROI for the spinal fusion mass included the mid-third region of the sample, also referred to as the central region (Supplementary Fig. S1). An average of three sections were quantified for each sample.

Statistical analysis

The primary outcome of the study was bone area% by histology defined as the percentage of bone tissue formed in the ROI of the spinal fusion mass or the transverse section of the intramuscular implants. Quantified data are reported as mean ± SD. Statistical analyses were conducted using GraphPad Prism 9 software. Normality was assessed using the Shapiro–Wilk test and one-way analysis of variance (ANOVA) with Tukey's *post hoc* test was used. A *p*-value of 0.05 was considered statistically significant.

Results

Inflammatory response towards microbial stimuli

To determine the rabbit response towards microbes, blood was stimulated *ex vivo* with different concentrations of the microbes. Cytokines, IL-6 and IL-1β, were measured as a general parameter for the proinflammatory response. A dose-dependent response was observed (Fig. 2). A significant

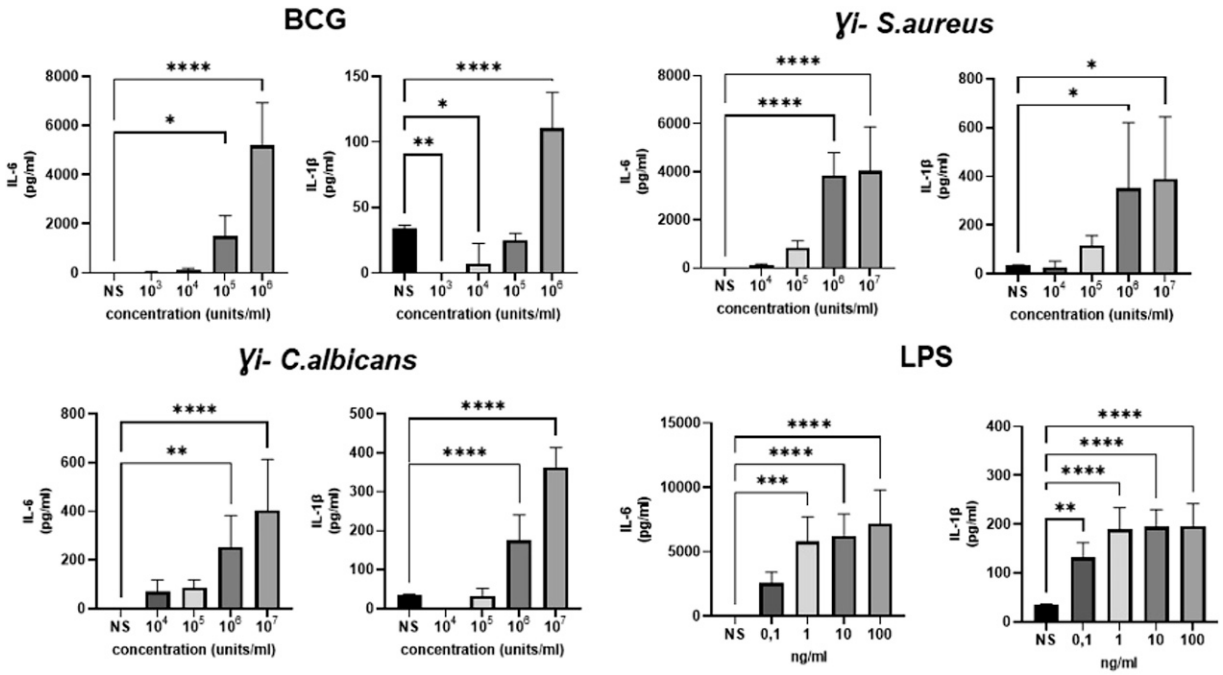

FIG. 2. IL-6 and IL-1β levels of rabbit blood stimulated *ex vivo* with BCG, γi-*S. aureus*, and γi-*C. albicans* for 24 h. LPS was included as a positive control. Data are depicted as mean ± SD ($n = 5$), NS, nonstimulated, $*p < 0.05$/$**p < 0.005$/$***p < 0.001$ one-way ANOVA with Tukey's *post hoc* test. BCG, Bacille Calmette–Guérin; γi-*S. aureus,* gamma-irradiated *Staphylococcus aureus*; LPS, lipopolysaccharide.

response was observed from a concentration of 1×10^5 units/mL for γi-*S. aureus* and BCG, while for γi-*C. albicans* a higher concentration of 1×10^6 units/mL was needed. Based on these results, high and low concentrations of 1×10^5 and 10^6 units/mL were used to prepare γi-*S. aureus* and BCG-treated implants, whereas 1×10^5 and 10^7 units/mL were used for the *C. albicans*-treated implants.

Spinal fusion mass analysis

All animals recovered well from surgery, except for one rabbit in the control group that did not recover from the anesthesia. This rabbit was euthanized and excluded from the analysis. Average temperature of the animals remained within normal limits (Supplementary Fig. S2A). All animals lost weight (7.4 ± 3.2% body weight) in the first week after surgery but gradually regained their weight and remained stable (Supplementary Fig. S2B). No prolonged systemic inflammation was observed demonstrated by comparable levels of CRP at weeks 3 post surgery with baseline (Supplementary Fig. S2C).

Gross inspection during necropsy showed granuloma tissue near the fusion mass in one animal of the γi-*C. albicans* group. As the fusion mass appeared normal, also by histology, we included it for analysis. One animal from the control group had intertransverse grafting on different levels and was therefore excluded from manual palpation. No other abnormalities were observed. Manual palpation indicated that all of the fusion levels were mobile, except for two out of six from the BCG group that were stiff. Micro-CT showed that remodeling of the transverse process occurred in all of the groups and new bone formed from the transverse process towards the center of the implant. In the best-performing sample of the BCG group, a clear bony bridge was observed from micro-CT (Fig. 3).

From histomorphometry analysis (Fig. 4), the average bone area percentage (bone area%) was highest in the BCG group (9 ± 4.4%) compared with the control (4.6 ± 2.3%). The best-performing sample in the BCG group (12.2% bone area) showed a complete bony bridge forming between the transverse processes, not observed in any other group. While the least performing sample (2% bone area) showed active bone remodeling in the transverse processes but hardly any bone in the central fusion mass. The spinal implants of the γi-*S. aureus* and γi-*C. albicans* groups had significantly lower bone area% in the central fusion mass compared with BCG, with an average of 1.4 ± 1.4% and 1.2 ± 0.6% respectively, which was also lower than the control. General observation of all the groups depicted a well-vascularized area with islands of new bone formation seen in the central region without direct contact with the transverse processes. Fluorochrome analysis showed positive labels at week 4 (oxytetracycline), week 7 (calcein green), and week 8 (xylenol orange) throughout the fusion mass (Fig. 4D), indicating that the onset of mineralization at the central fusion mass also occurred at an early time point by 4 weeks, suggestive of induction.

Intramuscular implant analysis

No new bone formation occurred in any of the ectopic implants implanted in the paraspinal muscles for 10 weeks. The pores of the BCP were filled with well-vascularized loose connective tissue and clustering of adipocyte cells forming marrow-like tissue was frequently observed (Fig. 5). There were no signs of inflammation.

Discussion

This study aimed to investigate the potential of microbial stimuli for enhancing bone formation in a rabbit PLF model. In addition, constructs were implanted intramuscularly to determine a potential osteoinductive effect. BCP with submicron needle-shaped topography was used as the scaffold,

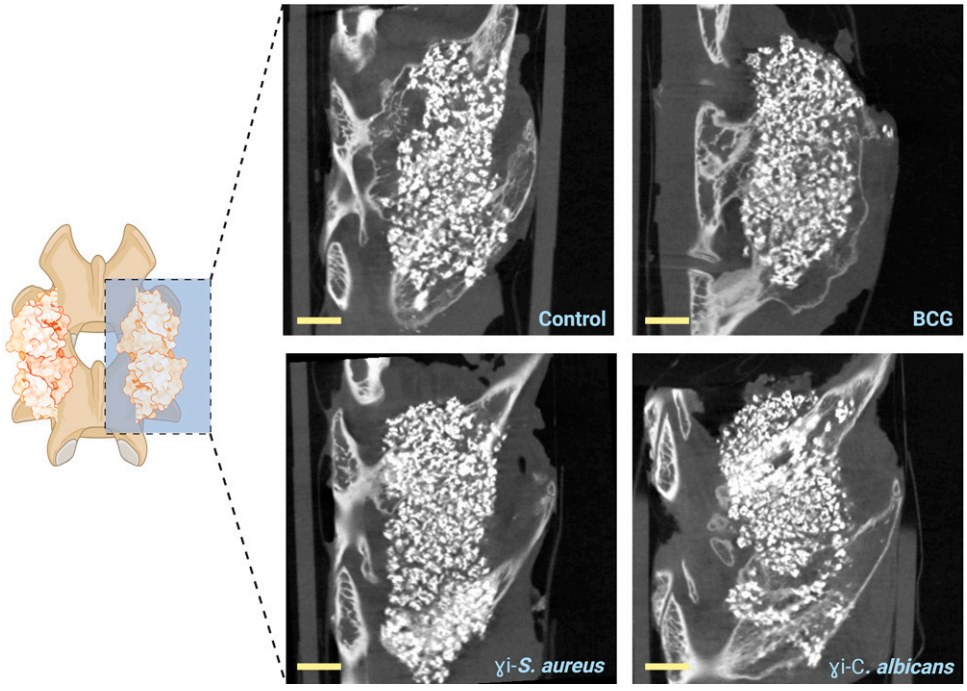

FIG. 3. Coronal micro-CT sections (voxel size 40 μm) of the PLF implants taken after 10 weeks. Images show remodeling of the transverse process (*in gray*) toward BCP granules (*in white*) and the formation of new bone tissue (*gray*) surrounding the granules. Images are of the best-performing sample of each group. Scale bar = 1 cm. PLF, posterolateral spinal fusion.

treated with either BCG, γi-*S. aureus*, or γi-*C. albicans*. The results of this study showed that immune stimuli influenced bone formation in the PLF model. Whereas γi-*S. aureus* and γi-*C. albicans* appeared to inhibit bone formation, and BCG stimulated bone formation with calcium phosphate granules.

The noninstrumented PLF model in rabbits is an established preclinical model for the evaluation of bone graft alternatives for spinal fusion.[26–28] The intended primary outcome of this model is fusion, defined as a continuous bony bridge between the transverse processes. Bone formation in the central area between the transverse processes is the most challenging achievement and is a minimal requirement for fusion between two adjacent transverse processes. The formation of bone in the fusion mass follows similar principles to fracture healing, with or without the initial cartilage template. Decortication of the transverse processes exposes the trabeculae and marrow, providing a source for new vasculature and progenitor cells,[32] whereas the BCP provides a scaffold for the conduction of bone growth. In our study, only two samples in the BCG group had a rigid fusion, as was confirmed by both manual palpation and micro-CT. No fusions occurred in any of the other groups. The control group demonstrates the performance of the BCP as a stand-alone graft material in this model. Although new bone tissue was observed in the central region of the fusion mass, suggestive of induction, no bony bridges were formed. The same BCP material was tested in a previous rabbit PLF model with complete fusion achieved at 12 weeks, but only when combined with autologous bone graft (1:1 ratio) as an enhancer.[25]

Compared with the control condition, γi-*S. aureus* or γi-*C. albicans* appeared to inhibit central bone formation. This may be due to inhibition of the osteoconductive process or less local bone induction. BCG however, showed more bone formation compared with the control. Altogether, these findings indicate that the inflammatory response induced by the immunomodulating compounds had an effect on local bone formation that was either inhibiting (γi-*S. aureus* or γi-*C. albicans*) or stimulative (BCG). A positive effect from BCG may be especially interesting for future investigations because of its widespread clinical use. BCG contains attenuated mycobacterium and is clinically applied as a vaccine against tuberculosis and as an immunomodulator for bladder cancer therapy. Repeated administration of BCG modifies the tumor microenvironment, making it more susceptible to T-helper and cytotoxic T-cell assaults.[33,34] There is also a possibility that the effects observed are model specific. In our previous studies, γi-*S. aureus* (1×10^9 units) led to significant thickening of bone cortex in a rabbit tibia model after 8 weeks, suggesting a pro-osteogenic effect,[22,23] which was not reproduced with the γi-*S. aureus* in the current PLF model. The dosage, time, and location of applying the inactive bacteria also contribute to the results found. The use of ectopic bone models to evaluate induction has been implemented in many locations, such as subcutaneous, intramuscular, and in the kidney capsule.[35] Among these, the intramuscular location offers distinct advantages. Muscles are well-vascularized organs and during muscle injury and regeneration, there is a natural upregulation of bone morphogenetic protein (BMP) signaling, transforming growth factor (TGF)-β1,[36] and insulin-like growth factor (IGF)-1,[37] which are part of both bone as well as skeletal muscle regeneration. Studies looking into earlier tissue response (within 2 weeks) observed that the type of cells aggregating within the pores of the ceramics impacts long-term tissue formation within the material.[4] This emphasizes the importance of the early inflammatory response that drives the localization of different cells into the implantation site and triggers their differentiation. Literature, however, has reported a high variation in the success of the ectopic implantation model and is largely influenced by the kind of animal used and the length of the implantation process.[38–41] In general, larger animals (such as goats, sheep, dogs, and baboons) and longer implantation periods have a higher likelihood of experiencing material-derived induction. It is still unclear why this phenomenon appears more frequently in larger animals than in smaller ones. A variety of physiological variations in metabolism, immune response, and muscle function are thought to be involved.[38–41] For intramuscular implantation in rabbits, many studies were performed with little success.[23,38,40,42,43] Only one study reported an average of 0.3% bone volume after 1 year of implantation.[38] This emphasizes that the current model with implantations for only 10 weeks is challenging. The absence of any sign of osteoinduction, even when higher concentrations of microbial stimuli were used, therefore should be interpreted within this context.

There are several limitations to this study. First, true rigid fusion was not determined by palpation, which questions the validity of the model for studying a clinically relevant endpoint. This may be the consequence of the relatively short 10-week follow-up. Fusion processes may continue beyond this period, and future investigations could explore longer follow-up durations to capture later-stage fusion events. Second is the constraint of measuring local inflammatory markers because the repository of antibodies, reagents, and resources to study the immune response in rabbits is limited. Finally, one could question the sample size of six animals in each group of the spinal fusion experiments. Literature reporting on the PLF model uses a range of 2–25 animals per group with a median sample size of 8 depending on the treatment used.[28] Future research should carefully evaluate the trade-offs between statistical power and practical constraints when designing future experiments.

FIG. 4. New bone formation within the BCP granules shown in undecalcified sections of specimens harvested from spinal implants after 10 weeks. **(A)** Basic fuchsin and methylene blue staining of sagittal sections showing the best and least performing fusion mass: bone (*pink*), scaffold (*dark brown/black*), fibrous tissue (*purple*). Insert shows bone in the central region of the fusion mass that has no direct contact with native bone. Scale bar: black = 5 mm; yellow = 100 μm. **(B)** Composition (%) of different structures in the ROI. **(C)** Detailed data of new bone formation (bone area%) in the ROI. Data are represented as mean ± SD ($n = 5–6$), $*p < 0.05$/$***p < 0.001$ one-way ANOVA with Tukey's *post hoc* test. **(D)** Microscopic images of fluorochrome labels administered at week 4 (oxytetracycline [O], *yellow*), week 7 (calcein green [C], *green*), and week 8 (xylenol orange [X], *red*). Sections of normal bone and the fusion mass show all three fluorochromes. Related bright field images show bone (B) and scaffold (S). Images are representative of each group. ROI, region of interest.

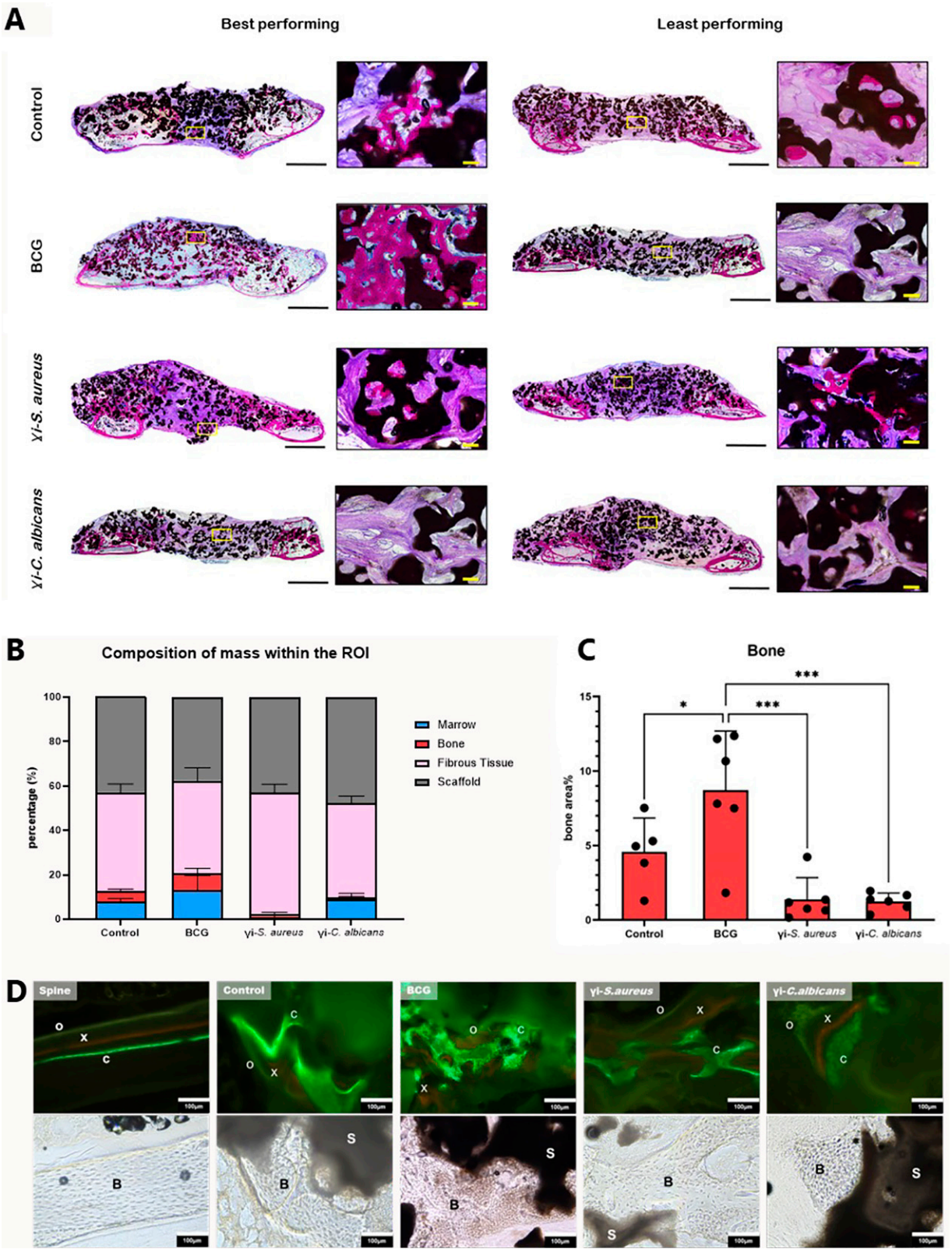

The use of microbe-derived agents in grafting procedures may raise concerns on the safety of such an approach. Our preference of using killed microbes in this explorative phase of research is derived from observations that killed microbes result in a balanced mix of pro- and anti-inflammatory cytokines, that may favor bone differentiation both *in vitro* and *in vivo*.[22,23,44] For future clinical translation, separate studies are conducted to investigate synthetically-derived microbial

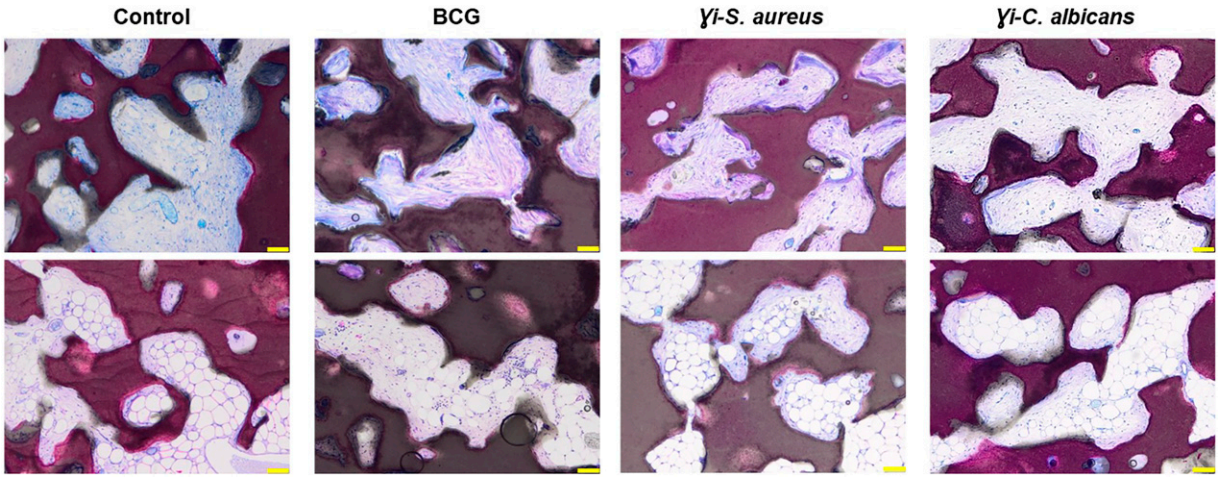

FIG. 5. Undecalcified sections of specimens harvested from intramuscular implantation after 10 weeks. Top images show fibrous tissue filling in the pores of the BCP and the bottom images show areas in which marrow-like tissue has formed. Images are representative of each group. Scale bars = 100 μm.

components recognized by the immune cells as pathogen-associated molecular patterns.[45–47]

Conclusion

This study showed promising results regarding the potential of microbial stimuli, especially BCG as an immunomodulatory adjuvant for bone regeneration. To date, there are no studies that link BCG and bone tissue regeneration and remodeling. Learning from the mechanism of action of BCG in other clinical use, we can speculate that the effects we observed on bone formation may be related to the initial inflammatory phase that affects cells of the adaptive immune system. While further research is needed, BCG presents a unique advantage as a medicinal product that is already widely used for its immunomodulatory effects in various clinical therapies.

Acknowledgments

Schematic illustrations in the article were created with Biorender.com.

Authors' Contributions

N.R.R., M.C., and M.C.K. designed the experiments. N.R.R., A.D., M.C., and O.L. conducted the experiments, interpreted, and analyzed the data. N.R.R. wrote the article. M.C.K. and H.W. secured the funding and contributed to the experiment design, data interpretation, and article review. A.D. and D.G. contributed to data interpretation and article review. All authors have read and approved the final submitted article.

Ethical Approval

Animal experiments (protocol number AVD11500020 16445) were reviewed and approved by the Central Authority for Scientific Procedures on Animals (Centrale Commissie Dierproeven [CCD], the Netherlands) and by the local animal ethics committee (Instantie voor Dierenwelzijn [IVD], Utrecht, the Netherlands).

Disclosure Statement

No competing financial interests exist.

Funding Information

This work is supported by PPS allowance from the Health ~ Holland LSH-TKI (grant no.: LSHM18011) and the EU's H2020 research and innovation program under Marie S. Curie Cofund RESCUE (grant agreement no. 801540).

Supplementary Material

Supplementary Figure S1
Supplementary Figure S2

References

1. Baldwin P, Li DJ, Auston DA, et al. Autograft, allograft, and bone graft substitutes: Clinical evidence and indications for use in the setting of orthopaedic trauma surgery. J Orthop Trauma 2019;33(4):203–213; doi: 10.1097/BOT.0000000000001420
2. Chai YC, Carlier A, Bolander J, et al. Current views on calcium phosphate osteogenicity and the translation into effective bone regeneration strategies. Acta Biomater 2012; 8(11):3876–3887; doi: 10.1016/j.actbio.2012.07.002
3. Lehr AM, Oner FC, Delawi D, et al. Dutch Clinical Spine Research Group. Efficacy of a standalone microporous ceramic versus autograft in instrumented posterolateral spinal fusion. Spine (Phila Pa 1976) 2020;45(14):944–951; doi: 10.1097/BRS.0000000000003440
4. Guo X, Li M, Qi W, et al. Serial cellular events in bone formation initiated by calcium phosphate ceramics. Acta Biomater 2021;134:730–743; doi: 10.1016/j.actbio.2021.07.037
5. van Dijk LA, Utomo L, Yuan H, et al. Calcium phosphate with submicron topography influences primary human macrophage response, enhancing downstream angiogenesis and osteogenesis *in vitro*. J Immunol Regen Med 2023;19: 100070; doi: 10.1016/j.regen.2023.100070
6. Li M, Guo X, Qi W, et al. Macrophage polarization plays roles in bone formation instructed by calcium phosphate

ceramics. J Mater Chem B 2020;8(9):1863–1877; doi: 10.1039/C9TB02932J
7. Duan R, Zhang Y, van Dijk L, et al. Coupling between macrophage phenotype, angiogenesis and bone formation by calcium phosphates. Mater Sci Eng C Mater Biol Appl 2021;122:111948; doi: 10.1016/j.msec.2021.111948
8. Montoya C, Du Y, Gianforcaro AL, et al. On the road to smart biomaterials for bone research: Definitions, concepts, advances, and outlook. Bone Res 2021;9(1):12–16; doi: 10.1038/s41413-020-00131-z
9. Lee J, Byun H, Perikamana SKM, et al. Current advances in immunomodulatory biomaterials for bone regeneration. Adv Healthcare Mater 2019;8(4):1801106; doi: 10.1002/adhm.201801106
10. Julier Z, Park AJ, Briquez PS, et al. Promoting tissue regeneration by modulating the immune system. Acta Biomater 2017;53:13–28; doi: 10.1016/j.actbio.2017.01.056
11. Davison NL, Gamblin AL, Layrolle P, et al. Liposomal clodronate inhibition of osteoclastogenesis and osteoinduction by submicrostructured beta-tricalcium phosphate. Biomate 2014;35(19):5088–5097; doi: 10.1016/j.biomaterials.2014.03.013
12. Friedenstein AY. Induction of bone tissue by transitional epithelium. Clin Orthop Relat Res 1968;59:21–37.
13. Mizuno K, Mineo K, Tachibana T, et al. The osteogenetic potential of fracture haematoma. Subperiosteal and intramuscular transplantation of the haematoma. J Bone Joint Surg Br 1990;72(5):822–829; doi: 10.1302/0301-620X.72B5.2211764
14. Michael S, Achilleos C, Panayiotou T, et al. Inflammation shapes stem cells and stemness during infection and beyond. Front Cell Dev Biol 2016;4:118; doi: 10.3389/fcell.2016.00118
15. Song G, Habibovic P, Bao C, et al. The homing of bone marrow MSCs to non-osseous sites for ectopic bone formation induced by osteoinductive calcium phosphate. Biomater 2013;34(9):2167–2176; doi: 10.1016/j.biomaterials.2012.12.010
16. Xu X, Zheng L, Yuan Q, et al. Transforming growth factor-β in stem cells and tissue homeostasis. Bone Res 2018;6(1):2–31; doi: 10.1038/s41413-017-0005-4
17. Linkhart TA, Mohan S, Baylink DJ. Growth factors for bone growth and repair: IGF, TGFβ and BMP. Bone 1996;19(1 Suppl):1S–12S; doi: 10.1016/S8756-3282(96)00138-X
18. Wahl SM, Wong H, McCartney-Francis N. Role of growth factors in inflammation and repair. J Cell Biochem 1989;40(2):193–199; doi: 10.1002/jcb.240400208
19. Ribatti D, Crivellato E. Immune cells and angiogenesis. J Cell Mol Med 2009;13(9a):2822–2833; doi: 10.1111/j.1582-4934.2009.00810.x
20. Goodman SB, Pajarinen J, Yao Z, et al. Inflammation and bone repair: From particle disease to tissue regeneration. Front Bioeng Biotechnol 2019;7:230; doi: 10.3389/fbioe.2019.00230
21. Maruyama M, Rhee C, Utsunomiya T, et al. Modulation of the inflammatory response and bone healing. Front Endocrinol (Lausanne) 2020;11:386; doi: 10.3389/fendo.2020.00386
22. Croes M, Boot W, Kruyt MC, et al. Inflammation-induced osteogenesis in a rabbit tibia model. Tissue Eng Part C Methods 2017;23(11):673–685; doi: 10.1089/ten.tec.2017.0151
23. Croes M, Kruyt MC, Boot W, et al. The role of bacterial stimuli in inflammation-driven bone formation. Eur Cell Mater 2019;37:402–419; doi: 10.22203/eCM.v037a24
24. Shi Y, Wang L, Niu Y, et al. Fungal component coating enhances titanium implant-bone integration. Adv Funct Mater 2018;28(46):1804483; doi: 10.1002/adfm.201804483
25. van Dijk LA, Barbieri D, Barrère-de Groot F, et al. Efficacy of a synthetic calcium phosphate with submicron surface topography as autograft extender in lapine posterolateral spinal fusion. J Biomed Mater Res B Appl Biomater 2019;107(6):2080–2090; doi: 10.1002/jbm.b.34301
26. Palumbo M, Valdes M, Robertson A, et al. Posterolateral intertransverse lumbar arthrodesis in the New Zealand white rabbit model: I. Surgical anatomy. Spine J 2004;4(3):287–292; doi: 10.1016/j.spinee.2003.11.004
27. Valdes M, Palumbo M, Appel AJ, et al. Posterolateral intertransverse lumbar arthrodesis in the New Zealand white rabbit model: II. Operative technique. Spine J 2004;4(3):293–299; doi: 10.1016/j.spinee.2003.08.022
28. Riordan AM, Rangarajan R, Balts JW, et al. Reliability of the rabbit postero-lateral spinal fusion model: A meta-analysis. J Orthop Res 2013;31(8):1261–1269; doi: 10.1002/jor.22359
29. Nguyen H, Morgan DAF, Forwood MR. Sterilization of allograft bone: Is 25 kGy the gold standard for gamma irradiation? Cell Tissue Bank 2007;8(2):81–91; doi: 10.1007/s10561-006-9019-7
30. Crowley JD, Oliver RA, Dan MJ, et al. Single level posterolateral lumbar fusion in a New Zealand white rabbit (Oryctolagus cuniculus) model: Surgical anatomy, operative technique, autograft fusion rates, and perioperative care. JOR Spine 2020;4(1):e1135; doi: 10.1002/jsp2.1135
31. Feiertag MA, Boden SD, Schimandle JH, et al. A rabbit model for nonunion of lumbar intertransverse process spine arthrodesis. Spine (Phila Pa 1976) 1996;21(1):27–31.
32. Craig Boatright K, Boden SD. JR., Biology of Spine Fusion. In: Bone Regeneration and Repair: Biology and Clinical Applications. (Lieberman JR, Friedlaender GE. eds) Humana Press: Totowa, NJ; 2005; pp. 225–239; doi: 10.1385/1-59259-863-3:225
33. Alexandroff AB, Jackson AM, O'Donnell MA, et al. BCG immunotherapy of bladder cancer: 20 years on. Lancet 1999;353(9165):1689–1694; doi: 10.1016/S0140-6736(98)07422-4
34. Pettenati C, Ingersoll MA. Mechanisms of BCG immunotherapy and its outlook for bladder cancer. Nat Rev Urol 2018;15(10):615–625; doi: 10.1038/s41585-018-0055-4
35. Scott MA, Levi B, Askarinam A, et al. Brief review of models of ectopic bone formation. Stem Cells Dev 2012;21(5):655–667; doi: 10.1089/scd.2011.0517
36. Smith CA, Stauber F, Waters C, et al. Transforming growth factor-β following skeletal muscle strain injury in rats. J Appl Physiol (1985) 2007;102(2):755–761; doi: 10.1152/japplphysiol.01503.2005
37. Mourkioti F, Rosenthal N. IGF-1, inflammation and stem cells: Interactions during muscle regeneration. Trends Immunol 2005;26(10):535–542; doi: 10.1016/j.it.2005.08.002
38. Cheng L, Wang T, Zhu J, et al. Osteoinduction of calcium phosphate ceramics in four kinds of animals for 1 Year: Dog, rabbit, rat, and mouse. Transplant Proc 2016;48(4):1309–1314; doi: 10.1016/j.transproceed.2015.09.065
39. Ripamonti U. Osteoinduction in porous hydroxyapatite implanted in heterotopic sites of different animal models. Biomater 1996;17(1):31–35; doi: 10.1016/0142-9612(96)80752-6
40. Yang Z, Yuan H, Tong W, et al. Osteogenesis in extraskeletally implanted porous calcium phosphate ceramics: Variability

among different kinds of animals. Biomater 1996;17(22): 2131–2137; doi: 10.1016/0142-9612(96)00044-0
41. Barradas AMC, Yuan H, Blitterswijk CAV, et al. Osteoinductive biomaterials: Current knowledge of properties, experimental models and biological mechanisms. Eur Cell Mater 2011;21:407–429; discussion 429; doi: 10.22203/ecm.v021a31.2011;21:407–429
42. Cheng L, Shi Y, Ye F, et al. Osteoinduction of calcium phosphate biomaterials in small animals. Mater Sci Eng C Mater Biol Appl 2013;33(3):1254–1260; doi: 10.1016/j.msec.2012.12.023
43. Croes M, Kruyt MC, Loozen L, et al. Local induction of inflammation affects bone formation. Eur Cell Mater 2017; 33:211–226; doi: 10.22203/eCM.v033a16
44. Rahmani NR, Belluomo R, Kruyt MC, et al. Trained innate immunity modulates osteoblast and osteoclast differentiation. Stem Cell Rev Rep 2024;20(4):1121–1134; doi: 10.1007/s12015-024-10711-9
45. Khokhani P, Warmink K, Kruyt MC, et al. Mixtures of Prr ligands partly mimic the immunomodulatory response of γi staphylococcus aureus, enhancing osteogenic differentiation of human mesenchymal stromal cells. SSRN 2024; doi: 10.2139/ssrn.4728625
46. Khokhani P, Rahmani NR, Kok A, et al. Use of therapeutic pathogen recognition receptor ligands for osteoimmunomodulation. Mater (Basel) 2021;14(5):1119; doi: 10.3390/ma14051119
47. Khokhani P, Belluomo R, Croes M, et al. An *in vitro* model to test the influence of immune cell secretome on mesenchymal stromal cell osteogenic differentiation. Tissue Eng Part C Methods 2022;28(8):420–430; doi: 10.1089/ten.tec.2022.0086

Address correspondence to:
Nada Ristya Rahmani, MD
Department of Orthopedics
University Medical Centre Utrecht
Heidelberglaan 100
G05.228, Utrecht 3508 GA
The Netherlands

E-mail: n.r.rahmani@umcutrecht.nl

Received: February 13, 2024
Accepted: June 11, 2024
Online Publication Date: October 29, 2024